Journal of Visualized Experiments

Measuring the pH, redox chemistries and degradative capacity of macropinosomes using dual-fluorophore ratiometric microscopy

--Manuscript Draft--

Article Type:	Invited Methods Article - JoVE Produced Video
Manuscript Number:	JoVE62733R2
Full Title:	Measuring the pH, redox chemistries and degradative capacity of macropinosomes using dual-fluorophore ratiometric microscopy
Corresponding Author:	Johnathan Canton, PhD University of Calgary - Faculty of Veterinary Medicine Calgary, AB CANADA
Corresponding Author's Institution:	University of Calgary - Faculty of Veterinary Medicine
Corresponding Author E-Mail:	johnathan.canton@ucalgary.ca
Order of Authors:	Liam Wilkinson
	Johnathan Canton, PhD
Additional Information:	
Question	**Response**
Please specify the section of the submitted manuscript.	Immunology and Infection
Please indicate whether this article will be Standard Access or Open Access.	Standard Access ($1400)
Please indicate the **city, state/province, and country** where this article will be **filmed**. Please do not use abbreviations.	Calgary, Alberta, Canada
Please confirm that you have read and agree to the terms and conditions of the author license agreement that applies below:	I agree to the Author License Agreement
Please provide any comments to the journal here.	
Please confirm that you have read and agree to the terms and conditions of the video release that applies below:	I agree to the Video Release

TITLE:

Measuring the pH, Redox Chemistries, and Degradative Capacity of Macropinosomes using Dual-Fluorophore Ratiometric Microscopy

AUTHORS AND AFFILIATIONS:

Liam Wilkinson[1,2], Johnathan Canton[2,3*]

[1]Department of Biochemistry & Microbiology, Faculty of Science, University of Victoria Victoria, BC V8P 5C2, Canada

[2]Department of Comparative Biology and Experimental Medicine, Faculty of Veterinary Science, University of Calgary, Calgary, AB T2N 4Z6, Canada

[3]Calvin, Joan and Phoebe Snyder Institute for Chronic Diseases, University of Calgary, Calgary, AB T2N 4Z6, Canada

Email addresses of co-authors:

Liam Wilkinson (lwilkinson220@gmail.com)

Johnathan Canton (johnathan.canton@ucalgary.ca)

[*]Corresponding Author:

Johnathan Canton (johnathan.canton@ucalgary.ca)

KEYWORDS:

macropinocytosis, macropinosome, endocytosis, pH, V-ATPase, proton pump, reactive oxygen species, ROS, NADPH oxidase, phagocyte, macrophage, dendritic cell

SUMMARY:

We describe protocols for measuring pH, oxidative events, and protein digestion in individual macropinosomes in live cells. An emphasis is placed on dual-fluorophore ratiometric microscopy and the advantages it offers over population-based techniques.

ABSTRACT:

In recent years, the field of macropinocytosis has grown rapidly. Macropinocytosis has emerged as a central mechanism by which innate immune cells maintain organismal homeostasis and immunity. Simultaneously, and in contrast to its homeostatic role, it can also drive various pathologies, including cancer and viral infections. Unlike other modes of endocytosis, the tools developed for studying the maturation of macropinosomes remain underdeveloped. Here the protocol describes newly developed tools for studying the redox environment within the lumen of early and maturing macropinosomes. Methodologies for using ratiometric fluorescence microscopy in assessing the pH, production of reactive oxygen species, and the degradative capacity within the lumen of individual macropinosomes in live cells are described. Single organelle measurements offer the advantage of revealing spatiotemporal heterogeneity, which is often lost with population-based approaches. Emphasis is placed on the basic principles of dual fluorophore ratiometric microscopy, including probe selection, instrumentation, calibration, and single-cell versus population-based methods.

INTRODUCTION:

Macropinocytosis refers to the uptake of large quantities of extracellular fluid into membrane-bound cytoplasmic organelles called macropinosomes[1,2]. It is a highly conserved process performed by free-living unicellular organisms, such as the amoeba *Dictyostelium spp*.[3], as well as anthozoans[4] and metazoans[2]. In most cells, macropinocytosis is an induced event. The ligation of cell-surface receptors induces the protrusion of actin-driven plasma membrane extensions referred to as ruffles. A fraction of those ruffles, by some poorly understood mechanism, seal at their distal tips to form macropinosomes (although beyond the scope of this methods paper, for detailed reviews on the mechanics of macropinocytosis, please refer to references[1,2,5,6,7]). The extracellular stimulus inducing macropinocytosis is most often a soluble growth factor[5,8]. Accordingly, the macropinocytic event allows for the ingestion of a bolus of extracellular material from which the cell can derive useful metabolites to facilitate growth. Unfortunately, this pathway for nutrient delivery can also drive pathology. Certain cancer cells harbor mutations that result in continuous or constitutive macropinocytosis. The continuous delivery of nutrients facilitates the uncontrolled proliferation of cancer cells and has been linked to particularly aggressive tumors[9–13]. Similarly, viruses can induce macropinocytosis to gain access to host cells, thereby driving viral pathology[14].

Macropinocytosis also functions in the maintenance of immunity to pathogens. Certain innate immune cells such as macrophages and dendritic cells engage in the constitutive and aggressive sampling of extracellular fluid via macropinocytosis[6,15,16]. This mode of macropinocytosis is incredibly active, and a single dendritic cell can engorge itself with a volume of extracellular fluid equivalent to its own weight every hour[17]. Despite this constitutive sampling, macrophages and dendritic cells do not replicate uncontrollably as do tumor cells, instead, they seem to process the extracellular material in such a way that information can be extracted to inform upon the presence, or indeed absence, of potential threats. Information is extracted as i) pathogen-associated molecular patterns that can be read by intracellular pathogen recognition receptors and ii) short stretches of amino acids that can be loaded onto major histocompatibility molecules for screening by cells of the adaptive immune system[16,18,19]. Whether pathogens subvert this pathway for information processing by immune cells is at present unclear.

Despite these well-defined and critical roles for macropinocytosis in both the maintenance of immunity and homeostasis and in contrast to other more commonly studied modes of endocytosis, little of the inner (luminal) workings of macropinosomes is known. Developing standardized protocols and tools to study the luminal biochemistry of macropinosomes will not only help us to understand their unique biology better but will provide insight that can be leveraged for novel therapeutic strategies, including drug delivery[20]. This method manuscript will focus on recently developed tools to dissect, at the single organelle level, various aspects of the luminal biochemistry of macropinosomes.

Fluorophores can be used to measure specific biochemistries of organelles if i) they partition preferentially into the compartment of interest and/or ii) they undergo spectral changes in response to the parameter of interest. For example, in the case of pH, fluorescent weak bases,

such as acridine orange, cresyl violet, and the LysoTracker dyes accumulate preferentially in acidic organelles. Therefore, their relative intensity is a rough indication that the labeled organelle is acidic. Other pH-responsive fluorophores, such as fluorescein, pHrodo, and cypHer5e, undergo spectral changes upon binding to protons (**Figure 1A–C**). Changes to the fluorescence emission of pH-sensitive fluorophores can therefore provide a useful approximation of pH. The use of single fluorophores, however, presents a number of disadvantages. For example, changes to the focal plane, photobleaching, and changes to the volume of individual organelles, a common occurrence in macropinosomes[21], can induce changes to the fluorescence intensity of single fluorophores, and this cannot be easily corrected for[22]. Single-wavelength assessments, although useful for visualizing acidic compartments, are therefore purely qualitative.

A more quantitative approach is to target the parameter-sensitive fluorophore along with a reference fluorophore to the organelle of interest. The reference fluorophore is ideally insensitive to biochemical changes within the organelle (**Figure 1D–F**) and can therefore be used to correct for changes in the focal plane, organellar volume, and, to some extent, photobleaching[23]. Using this approach, referred to as dual-fluorophore ratiometric fluorescence, correction can be achieved by generating a ratio of the fluorescence emission of the parameter-sensitive fluorophore to the reference fluorophore.

Here, the protocol will be utilizing the principle of dual-fluorophore ratiometric imaging to measure pH, oxidative events, and protein degradation within macropinosomes. In each case, a fluorophore will be selected that is sensitive to the parameter of interest and a reference fluorophore. In order to target the fluorophores specifically to macropinosomes, they will be covalently coupled to 70 kDa dextran, which is preferentially incorporated into macropinosomes[24]. All assays will be performed in Raw264.7 cells but can be adapted to other cell types. Where possible, the fluorescence ratios will be calibrated against a reference curve to gain absolute values. Importantly, all measurements will be performed in live cells for dynamic and quantitative assessment of the luminal environment of macropinosomes.

When selecting pH-sensitive fluorophores, a number of considerations must be weighed. The first is the pK_a of the fluorophore, which indicates the range of pH values at which the probe will be most sensitive. If it is assumed that shortly after formation, the pH of the macropinosome will be close to that of the extracellular medium (~pH 7.2) and that it will progressively acidify through interactions with late endosomes and lysosomes (~pH 5.0), then a probe with a pK_a that is sensitive within that range (**Figure 2C**) should be selected. The fluorophore fluorescein, which has a pK_a of 6.4, is optimally sensitive within that range. It has been used extensively to measure other similar organelles, such as phagosomes, and will be the fluorophore of choice in this manuscript[22,25]. As a reference fluorophore, tetramethylrhodamine will be used, which is insensitive to pH (**Figure 1E**). Other fluorophores, such as pHrodo and cypHer5e may be substituted for fluorescein where the spectral properties of fluorescein do match other experimental variables. Some suggested reference fluorophores for pHrodo and cypHer5e are shown in **Figure 1**.

A second consideration is the method by which the two fluorophores will be targeted specifically to macropinosomes. Dextran of the size 70 kDa, which has a hydrodynamic radius of roughly 7 nm, does not stick non-specifically to cells and is incorporated into macropinosomes, but not clathrin-coated pits or caveolae, and therefore marks macropinosomes (**Figure 2A** and **Figure 3A,B**)[16,24,26]. In this protocol, fluorescein-labeled 70 kDa dextran and tetramethylrhodamine (TMR)-labeled 70 kDa dextran will be used as the pH-sensitive and reference probes, respectively.

In innate immune cells, macropinocytosis and phagocytosis represent the two major routes for the internalization of exogenous material for processing and subsequent presentation to cells of the adaptive immune response[27]. The careful and coordinated control of the redox chemistry of the lumen of phagosomes and macropinosomes is critical to the context-specific processing of exogenous material. Perhaps the most well-studied regulator of oxidative events in phagosomes is the NADPH oxidase, a large multi-subunit complex that produces large quantities of reactive oxygen species (ROS) within the lumen of phagosomes[28]. Indeed, its activity is central to appropriate antigen processing within phagosomes[29,30]. Yet, the activity of the NADPH oxidase on macropinosomal membranes has not been explored.

In this protocol, the H2DCFDA succinimidyl ester is used for measuring oxidative events within the macropinosome. This is a modified form of fluorescein (2',7'-dichlorodihydrofluorescein diacetate), which is minimally fluorescent in its reduced form. Upon oxidation, its fluorescence emission increases significantly. It is, however, worth noting a significant caveat of H2DCFDA – as it is based on the fluorophore fluorescein, its fluorescence is also quenched in acidic compartments, and care must be taken to control for this variable when designing experiments[28]. Similar to the approach for measuring pH, the H2DCFDA succinimidyl ester will be covalently attached to 70 kDa dextran and TMR-labeled 70 kDa dextran will be used as the reference fluorophore (**Figure 3A**).

Fluorescent ovalbumin will be used to measure protein degradation within macropinosomes. The ovalbumin used here is densely labeled with a 4,4-difluoro-4-bora-3a,4a-diaza-s-indacene (BODIPY) FL dye that is self-quenched. Upon digestion, strongly fluorescent dye-labeled peptides are liberated. As ovalbumin cannot be easily conjugated to 70 kDa dextran, cells with TMR-labeled 70 kDa dextran and fluid-phase ovalbumin will be co-incubated. The TMR signal will be used to generate a macropinosome mask during post-imaging analysis, and the signal liberated from the digested ovalbumin will be measured within the mask (**Figure 3B**).

PROTOCOL:

1. Preparation of cells

1.1. Grow Raw264.7 cells at 37 °C and 5% CO_2 to 70% confluency in RPMI supplemented with 10% heat-inactivated serum.

1.2. One day before the assay, seed Raw264.7 cells at a density of 5 x 10^4 cells per well in a 96-well plate. Ensure that each well contains 100 μL of growth medium. Ensure that the 96-well plate has black sides and a glass-bottom for imaging.

NOTE: Here, 96-well plates were used for imaging. The 96-well plates allow for the use of smaller quantities of cells and reagents relative to larger imaging chambers. However, any chamber designed for imaging live cells can be used, and reagents can be scaled up accordingly.

1.3. On the day of the assay, check whether the wells are at least 70% confluent.

2. Measuring macropinosome pH

2.1. Prepare the cells as in section 1.

2.2. Wash all the wells with 100 μL of HBSS at 37 °C.

2.3. Fill each well with 100 μL of HBSS containing 0.025 mg/mL of TMR-labeled 70 kDa dextran and 0.025 mg/mL of fluorescein-labeled 70 kDa dextran.

2.4. Place the cells into an incubator set to 37 °C for 15 min.

2.5. Remove the cells from the incubator and wash the cells 6x with 100 μL of HBSS.

2.6. Fill each well with 100 μL of HBSS at 37 °C.

2.7. Place the plate on the microscope with a heated stage and chamber.

2.8. Adjust the excitation/emission parameters for each fluorophore as needed.

NOTE: Ideal conditions for image acquisition will vary with fluorophores used and individual microscope set-ups. Here, images were acquired on a Leica SP5 laser scanning confocal microscope. TMR was excited with a 543-laser line and emission was collected from 610 nm to 650 nm. Fluorescein was excited with a 488-laser line and emission was collected from 500 nm to 550 nm. A 63x oil immersion objective was used and a 10 μm Z-volume was acquired at 0.5 μm intervals.

2.9. Acquire an image from each well, alternating between fluorophores in between each well.

2.10. After the first acquisition, check whether all the wells remained in focus across the entire plate.

2.11. Acquire images of each well at 1–15 min intervals for the desired length of time.

3. *In situ* calibration of macropinosome pH

3.1. During the image acquisition, prepare 1 L of potassium-rich (K^+-rich) solution containing 140 mM KCl, 1 mM $MgCl_2$, 1 mM $CaCl_2$, and 5 mM glucose. Supplement one 400 mL volume of the K^+-rich solution with 25 mM HEPES (from a 1 M, pH 7.2 stock solution) and a separate 400 mL volume with 25 mM MES (from a 0.5 M, pH 6.0 stock solution).

3.2. Adjust a 50 mL aliquot of the K^+-rich solution buffered with 25mM HEPES to pH 7.5 using 10 M HCl or 10 M KOH as needed.

3.3. Adjust three separate 50 mL aliquots of the K^+-rich solution buffered with 25mM MES to pH 6.5, pH 5.5, and pH 5.0 using 10 M HCl or 10 M KOH as needed.

NOTE: An acetate-acetic acid buffer may be preferable for lower pH solutions.

3.4. After the completion of image acquisition, remove the HBSS from the 96-well plate containing the cells and replace it with the K^+-rich solution that is at pH 7.5.

3.5. Add nigericin to a final concentration of 10 μg/mL.

NOTE: Nigericin is an ionophore that exchanges K^+ for H^+. By setting the K^+ concentration of the K^+-rich solution to a value that approximates the K^+ concentration of the cytosol, it can be ensured that nigericin will clamp the pH of the macropinosome to that of the cytosol, which in turn reflects the pH of the calibration buffer.

3.6. Place the plate back on the microscope and acquire images of each well using the same acquisition settings as above.

3.7. Repeat steps 3.5 and 3.6 for each calibration buffer.

4. Data analysis for macropinosome pH

4.1. Using FIJI software, subtract the background from both the TMR and the fluorescein channel.

4.2. Generate a mask on the TMR channel. To generate a mask, convert the image to a binary image by selecting **Adjust** > **Threshold** > **Apply**. Next, highlight the binary image and select **Edit** > **Selection** > **Create Mask**.

4.3. Apply it to both the TMR and fluorescein images. To do this, highlight the mask and select **Edit** > **Selection** > **Create Selection**. Click on the TMR image and press **Shift + E** to apply the mask to the TMR channel. Similarly, click on the fluorescein image and press **Shift + E** to apply the mask to the OB channel.

4.4. Record the TMR and fluorescein intensity for each macropinosome within the masks.

4.5. Repeat steps 4.1–4.3 for each time point from the time course.

4.6. Repeat steps 4.1–4.3 for the images captured in the *in situ* calibration.

4.7. Divide the fluorescein intensity by the TMR intensity to generate the fluorescein:TMR ratio.

4.8. Plot the pH against the fluorescein:TMR ratios for the calibration images.

4.9. Fit a curve to the calibration data.

4.10. Interpolate the data for each time point from the time course to get absolute pH values.

5. Measuring oxidative events within macropinosomes

5.1. Prepare the cells as in section 1.

5.2. One day before the assay, prepare the H2DCFDA succinimidyl ester labeled 70 kDa dextran by resuspending 10 mg of 70 kDa dextran-amino in 1 mL of 0.1 M sodium bicarbonate solution (pH 8.3). Add 1 mg of the H2DCFDA succinimidyl ester to the dextran-amino solution and incubate for 1 h. Dialyze the H2DCFDA-labeled 70 kDa dextran against PBS. Do not store for more than 1 day as H2DCFDA-labeled 70 kDa dextran will oxidize upon storage.

5.3. On the day of the assay, wash all the wells with 100 µL of HBSS at 37 °C.

5.4. Fill each well with 100 µL of HBSS containing 0.025 mg/mL of TMR-labeled 70 kDa dextran and 0.025 mg/mL of H2DCFDA-labeled 70 kDa dextran.

5.5. Place cells into an incubator set to 37 °C for 15 min.

5.6. Remove cells from the incubator and wash the cells 6x with 100 µL of HBSS.

5.7. Fill each well with 100 µL of HBSS at 37 °C.

5.8. Place the plate on the microscope with a heated stage and chamber and adjust the excitation/emission parameters for each fluorophore as needed.

NOTE: Ideal conditions for image acquisition will vary with fluorophores used and individual microscope set-ups. Here images were acquired on a Leica SP5 laser scanning confocal microscope. TMR was excited with a 543-laser line, and emission was collected from 610 nm to 650 nm. H2DCFDA was excited with a 488-laser line and emission was collected from 500 nm to

550 nm. A 63x oil immersion objective was used, and a 10 μm Z-volume was acquired at 0.5 μm intervals.

5.9. Acquire an image from each well, alternating between fluorophores in between each well.

5.10. After the first acquisition, check whether all the wells remain in focus across the entire plate.

5.11. Acquire images of each well at 1–15 min intervals for the desired length of time.

6. Data analysis for oxidative events within macropinosomes

6.1. Using FIJI software, subtract the background from both the TMR and H2DCFDA channels.

6.2. Generate a mask on the TMR channel. To generate a mask, convert the image to a binary image by selecting **Adjust** > **Threshold** > **Apply**. Next, highlight the binary image and select **Edit** > **Selection** > **Create Mask**.

6.3. Apply the mask to both the TMR and H2DCFDA images. To do this, highlight the mask and select **Edit** > **Selection** > **Create Selection**. Click on the TMR image and press **Shift + E** to apply the mask to the TMR channel. Similarly, click on the H2DCFDA image and press **Shift + E** to apply the mask to the H2DCFDA channel.

6.4. Record the TMR and H2DCFDA intensity for each macropinosome within the masks.

6.5. Repeat steps 4.1–4.3 for each time point from the time course.

6.6. Divide the H2DCFDA intensity by the TMR intensity to generate an H2DCFDA: TMR ratio.

6.7. Plot the H2DCFDA: TMR ratio against time.

7. Measuring protein digestion within macropinosomes

7.1. Prepare the cells as in section 1.

7.2. On the day of the assay, wash all the wells with 100 μL HBSS at 37 °C.

7.3. Dissolve BODIPY-labeled ovalbumin to a concentration of 4 mg/mL in HBSS.

7.4. Fill each well with 100 μL of HBSS containing 0.025 mg/mL of TMR-labeled 70 kDa dextran and 0.2 mg/mL of BODIPY-labeled ovalbumin.

7.5. Place the cells into an incubator set to 37 °C for 15 min.

7.6. Remove cells from the incubator and wash the cells 6x with 100 μL of HBSS.

7.7. Fill each well with 100 μL of HBSS at 37 °C.

7.8. Place the plate on the microscope with a heated stage and chamber and adjust the excitation/emission parameters for each fluorophore as needed.

NOTE: Ideal conditions for image acquisition will vary with fluorophores used and individual microscope set-ups. Here, images were acquired on a Leica SP5 laser scanning confocal microscope. TMR was excited with a 543-laser line, and emission was collected from 610 nm to 650 nm. BODIPY was excited with a 488-laser line, and emission was collected from 500 nm to 550 nm. A 63x oil immersion objective was used and a 10 μm Z-volume was acquired at 0.5 μm intervals.

7.9. Acquire an image from each well, alternating between fluorophores in between each well.

7.10. After the first acquisition, check whether all the wells remain in focus across the entire plate.

7.11. Acquire images of each well at 1–15 min intervals for the desired length of time.

8. Data analysis for protein digestion within macropinosomes

8.1. Using FIJI software, subtract the background from both the TMR and BODIPY channels.

8.2. Generate a mask on the TMR channel and apply it to both the TMR and BODIPY images as in steps 6.2 and 6.3 above (**Figure 3B**).

8.3. Record the TMR and BODIPY intensity for each macropinosome within the masks.

8.4. Repeat steps 4.1–4.3 for each time point from the time course.

8.5. Divide the BODIPY intensity by the TMR intensity to generate the BODIPY:TMR ratio.

8.6. Plot the BODIPY:TMR ratio against time.

REPRESENTATIVE RESULTS:

When measuring macropinosome pH, there is a period of time for which the dynamics of acidification cannot be measured. This period corresponds to the dextran loading phase (gray box in **Figure 2C** and **Figure 3C**,**D**) and will vary depending on the cell type used. The length of the loading phase will vary with (i) the macropinocytic activity of the cells and (ii) the sensitivity of the instrument used. It is recommended to adjust this period at the start of each experiment such that a signal:noise ratio of greater than 4:1 is achieved for both the fluorescein and the TMR channels. In untreated cells, the fluorescein emission should become progressively weaker as the

macropinosomes acidify, and the TMR signal should remain either constant or become brighter. The TMR signal may become brighter if the macropinosomes shrink in size[16,21]. This will not affect the ratio as the fluorescein signal is subject to the same variations in organellar size[22]. The fluorescein:TMR ratio will become progressively smaller and will plateau within the first 15 min of acquisition (**Figure 2C**). This plateau corresponds to a pH of ~5, which roughly matches the pH of lysosomes[25]. At the end of each acquisition, an *in situ* calibration is performed. The fluorescein:TMR ratio should be largest with the calibration buffer at pH 7.5 and become progressively smaller as the calibration buffers become more acidic. This allows for the generation of a calibration curve (**Figure 2B**). The fluorescein:TMR ratios can then be interpolated for macropinosomal pH (**Figure 2C**).

Oxidative events within macropinosomes are also likely to vary with the cell type being used. It is recommended to load the cells with H2DCFDA-dextran, and to stimulate the NADPH oxidase using phorbol 12-myristate 13-acetate (PMA) as a positive control (**Figure 3C**). This will give a better idea of the dynamic range of the assay and will allow for adjustment of the microscope settings. As oxidative events occur within the macropinosomes, the H2DCFDA signal will become progressively brighter. The TMR signal may remain constant or may vary with the size of macropinosome, as discussed above. The ratio of H2DCFDA:TMR will become progressively larger and will likely plateau within the first 20–30 min in inactivated Raw264.7 cells (**Figure 3A**,**C**).

When measuring macropinosomal protein digestion, a progressively strong fluorescent signal will be liberated as the ovalbumin is digested. In Raw264.7 cells, the increase in fluorescence liberated from the digested BODIPY-labeled ovalbumin will plateau within the first 30 min (**Figure 3B,D**). As before, the TMR signal may remain constant or may vary with size of macropinosome. As degradation of ovalbumin begins immediately after the macropinosome closure, a negative control can be useful in determining the dynamic range of the assay. To this end, acid hydrolases within the macropinosome can be inhibited using an inhibitor of the V-ATPase, such as Concanamycin A (CcA) (**Figure 3D**) or Bafilomycin A.

FIGURE AND TABLE LEGENDS:

Figure 1: Principles of dual-fluorophore ratiometric imaging. (**A–C**). Spectral scans (excitation-fixed, emission-varied) of pH-sensitive fluorophores suspended in buffers of the indicated pH. Fluorescein, pHrodo, and cypHer5e are commonly used as sensors of pH in cellular assays. (**D–F**). Spectral scans (excitation-fixed, emission-varied) of pH-insensitive fluorophores suspended in buffers of the indicated pH. Dyes that do not vary with pH make useful reference fluorophores. Fluorescein, are not optimally sensitive at the more acidic pH values experienced in endosomes.

Figure 2: Dynamic measurements of macropinosomal pH. (**A**) Raw264.7 cells were loaded with with fluorescein-labeled 70 kDa dextran and TMR-labeled 70 kDa dextran at 37 °C in the presence or absence of 500 ng/mL of Lipopolysaccharide (LPS) for 15 min. They were also incubated with fluorescein-labeled 70 kDa dextran and TMR-labeled 70 kDa dextran at 4 °C as a control for the non-specific binding of dextran. Insets show individual cells (Scale bars = 20 μm). (**B**) *In situ* calibration of Raw264.7 cells loaded with fluorescein-labeled 70 kDa dextran and TMR-labeled 70 kDa dextran using K^+-rich buffers at the indicated pH and nigericin. (**C**) Macropinosome pH in

Raw264.7 cells. Insets represent the fluorescein:TMR ratio in individual macropinosomes. Gray boxes indicate the times when cells were being loaded with dextran. Data from two independent experiments each containing ≥ 80 cells. Data represented as mean ± SEM.

Figure 3: Dynamic measurements of oxidative events and protein digestion within the lumen of macropinosomes. (**A**) Raw264.7 cells were loaded with H2DCFDA-labeled 70 kDa dextran and TMR-labeled 70 kDa dextran at 37 °C for 15 min, followed by a 45 min chase at 37 °C. Insets show ratioed images (H2DCFDA/TMR) of individual macropinosomes. Scale bars = 20 μm. (**B**) Raw264.7 cells were loaded with BODIPY-labeled ovalbumin and TMR-labeled 70 kDa dextran at 37 °C for 15 min, followed by a 45 min chase at 37 °C. The TMR channel was used to generate a mask, which was applied to the BODIPY channel. Insets show individual cells. Scale bars = 20 μm. (**C**) H2DCFDA oxidation within the lumen of macropinosomes. Cells were also stimulated with PMA as a positive control. Gray boxes indicate the times when cells were being loaded with dextran. Data from two independent experiments, each containing ≥ 80 cells. Data represented as mean ± SEM. Each time point was compared to the PMA control. A student's *t*-test was used for statistical analysis. (**D**) BODIPY-labeled ovalbumin degradation within macropinosomes. Concanamycin A (CcA) was used as a negative control as it prevents the activation of luminal acid hydrolases. Data from two independent experiments, each containing ≥ 80 cells. Data represented as mean ± SEM. Each time point was compared to the CcA control. A student's *t*-test was used for statistical analysis.

DISCUSSION:

Although there are a number of protocols for both low and high-throughput measurements of macropinocytic uptake in macrophages, fibroblasts, and even *Dictyostelium spp.*[3,7,31–33], very few attempts have been made to measure the luminal biochemistry of these dynamic compartments. This is likely due to a paucity of probes that can be efficiently targeted to the macropinosomal compartment while avoiding other endocytic compartments. Described here are the techniques to target fluorescent probes for the dynamic measurement of pH, oxidative events, and protein digestion within macropinosomes.

Ratiometric fluorescence microscopy has been the primary technique by which endosomal pH has been measured for decades. Fluorescein has been widely used for measuring endosomal pH and continues to be the fluorophore of choice as its pK_a allows for accurate measurements with the typical range of endosomal pH values (~pH 7.2–4.5). Here, the study employed fluorescein conjugated to 70 kDa dextran for macropinosome-specific pH measurements. A limitation of this approach is the 15 min dextran loading period during which macropinosomal pH cannot be recorded. This period is required to load sufficient fluorophore-labeled dextran into the macropinosomal compartment but effectively precludes early macropinosome pH measurements. This does not, however, preclude determinations of various luminal parameters such as the buffering capacity, relative proton leak, and V-ATPase pumping power, all of which are derived from macropinosomal pH measurements. As shown in **Figure 1**, a number of other pH-sensitive fluorophores may also be used to measure pH, including pHrodo (pK_a = 6.8) and

CypHer5e (pK_a = 7.3). However, as they have a significantly higher pK_a than fluorescein, they are not optimal for measuring endosomal pH at more acidic pH values.

As macropinosomes are highly dynamic organelles and undergo significant shrinkage shortly after forming[16,21], dual-fluorophore ratiometric fluorescence is required. Changes in fluorescence due to changes in the volume of macropinosomes are corrected for using a reference fluorophore in all of the assays presented.

Oxidative events in cells have been measured using a variety of redox-sensitive probes, including nitroblue tetrazolium (NBT), luminol, and H2DCFDA. Luminol-based approaches are particularly useful for measuring ROS production in a population of cells but are difficult to adapt to organelle-specific measurements. NBT forms an easily visualized insoluble deposit called formazan upon oxidation but obscures fluorescent signals and is both nonlinear and difficult to localize. H2DCFDA liberates a linear fluorescent signal upon oxidation and can be readily conjugated to tracers such as dextran for organelle-specific measurements. By attaching H2DCFDA to 70 kDa dextran, oxidative events within individual macropinosomes (**Figure 3B**) can be visualized. There is, however, a caveat to this approach. As H2DCFDA is a modified form of fluorescein, the signal liberated is pH sensitive. Although the gain in fluorescence upon oxidation is large enough to be detected, it is undoubtedly masked by the acidic lumen of the macropinosome. A pH-insensitive variant of H2DCFDA has been previously commercially available and is preferable; however, at the time of preparing this manuscript, this product was no longer commercially available. ROS is emerging as an important signaling molecule and has been implicated in membrane remodeling, organellar trafficking, and more recently in the processing of the material by antigen-presenting cells for presentation to T cells[28,30]. The method presented here can be used to study the contribution of macropinosomal ROS production to these various physiological processes.

Protein digestion in macropinosomes is of interest in the study of antigen presentation by immune cells as well as the study of nutrient acquisition by cancer cells. For example, endosomal protein digestion by dendritic cells is believed to limit the pool of peptides available for presentation to T cells on major histocompatibility molecules. As macropinosomes are a major route of antigen acquisition, measurements of macropinosomal protein digestion may be used to probe the molecular machinery responsible for fine-tuning antigen presentation. A number of commercially available tools are used for measuring protein digestion in endosomal compartments. The BODIPY-labeled BSA and ovalbumin probes, which become strongly fluorescent upon digestion, have proven particularly popular. They are easily coupled to endocytic tracers and can be targeted to specific endosomal compartments, such as phagosomes. The probes, however, are not readily coupled to dextran and so require a co-localization approach. This approach results in the loading of all endosomal compartments, including macropinosomes, with BODIPY-labeled ovalbumin, and a mask is used to measure the macropinosome-specific degradation. This approach requires better resolution and is not easily scaled up for larger, more high throughput analyses. Techniques to covalently couple protein degradation tools to 70 kDa dextran will likely prove useful and are currently being developed in our laboratory.

As the field of macropinocytosis continues to grow[34], tools for dynamically measuring the luminal biochemistry of macropinosomes, including pH, redox chemistries, protein digestion, ion concentrations, and lipid chemistries will provide insight into the unique biology of these rapidly evolving organelles.

DISCLOSURES:

The authors have no conflicts of interest to disclose.

ACKNOWLEDGMENTS:

We thank the University of Calgary for its support. We would also like to thank Dr. Robin Yates for access to reagents, equipment, and useful discussions.

REFERENCES:

1. Canton, J. Macropinocytosis: New insights into its underappreciated role in innate immune cell surveillance. *Frontiers in Immunology*. **9** (2018).
2. Marques, P. E., Grinstein, S., Freeman, S. A. SnapShot: Macropinocytosis. *Cell*. **169**, 766–766.e1 (2017).
3. Williams, T., Kay, R. R. High-throughput measurement of Dictyostelium discoideum macropinocytosis by flow cytometry. *Journal of Visualized Experiments: JoVE*. **139**, 58434 (2018).
4. Ganot P. et al. Ubiquitous macropinocytosis in anthozoans. *eLife*. **50022** (2020).
5. Charpentier, J. C. et al. Macropinocytosis drives T cell growth by sustaining the activation of mTORC1. *Nature Communications*. **11**, 180 (2020).
6. Bohdanowicz, M. et al. Phosphatidic acid is required for the constitutive ruffling and macropinocytosis of phagocytes. *Molecular Biology of the Cell*. **24**, 1700–1712 (2013).
7. Commisso, C., Flinn, R. J., Bar-Sagi, D. Determining the macropinocytic index of cells through a quantitative image-based assay. *Nature Protocols*. **9**, 182–192 (2014).
8. Yoshida, S., Pacitto, R., Sesi, C., Kotula, L., Swanson, J. A. Dorsal ruffles enhance activation of Akt by growth factors. *Journal of Cell Science*. **131** (2018).
9. Commisso, C. et al. Macropinocytosis of protein is an amino acid supply route in Ras-transformed cells. *Nature*. **497**, 633–637 (2013).
10. Commisso, C. The pervasiveness of macropinocytosis in oncological malignancies. *Philosophical Transactions of the Royal Society of London B Biological Sciences*. **374**, 20180153 (2019).
11. Zhang, Y. et al. Macropinocytosis in cancer-associated fibroblasts is dependent on CaMKK2/ARHGEF2 signaling and functions to support tumor and stromal cell fitness. *Cancer Discovery*. candisc.0119.2020 (2021).
12. Lee, S.-W. et al. EGFR-Pak signaling selectively regulates glutamine deprivation-induced macropinocytosis. *Developmental Cell*. **50**, 381–392.e5 (2019).
13. Michalopoulou, E. et al. Macropinocytosis renders a subset of pancreatic tumor cells resistant to mTOR inhibition. *Cell Reports*. **30**, 2729–2742.e4 (2020).
14. Mercer, J., Helenius, A. Virus entry by macropinocytosis. *Nature Cell Biology*. **11**, 510–520 (2009).

15. West, M. A. et al. Enhanced dendritic cell antigen capture via toll-like receptor-induced actin remodeling. *Science*. **305**, 1153–1157 (2004).
16. Canton, J. et al. Calcium-sensing receptors signal constitutive macropinocytosis and facilitate the uptake of NOD2 ligands in macrophages. *Nature Communications*. **7**, 11284 (2016).
17. Sallusto, F., Cella, M., Danieli, C., Lanzavecchia, A. Dendritic cells use macropinocytosis and the mannose receptor to concentrate macromolecules in the major histocomaptibility complex class II compartment: downregulation by cytokines and bacterial products. *Journal of Experimental Medicine*. **182**, 389–400 (1995).
18. Bhosle, V. K. et al. SLIT2/ROBO1-signaling inhibits macropinocytosis by opposing cortical cytoskeletal remodeling. *Nature Communications*. **11**, 4112 (2020).
19. Liu, Z., Roche, P. A. Macropinocytosis in phagocytes: regulation of MHC class-II-restricted antigen presentation in dendritic cells. *Frontiers in Physiology*. **6**, 1 (2015).
20. Desai, A. S., Hunter, M. R., Kapustin, A. N. Using macropinocytosis for intracellular delivery of therapeutic nucleic acids to tumour cells. *Philosophical Transactions of the Royal Society of London B. Biological Sciences*. **374**,20180156 (2019).
21. Freeman, S. A. et al. Lipid-gated monovalent ion fluxes regulate endocytic traffic and support immune surveillance. *Science*. **367**, 301–305 (2020).
22. Canton, J., Grinstein, S. Measuring phagosomal pH by fluorescence microscopy. *Methods in Molecular Biology Clifton NJ*. **1519**, 185–199 (2017).
23. Cheung, S., Greene, C., Yates, R. M. Simultaneous analysis of multiple lumenal parameters of individual phagosomes using high-content imaging. *Methods Molecular Biology Clifton NJ*. **1519**, 227–239 (2017).
24. Li, L. et al. The effect of the size of fluorescent dextran on its endocytic pathway. *Cell Biology International*. **39**, 531–539 (2015).
25. Canton, J., Grinstein, S. Measuring lysosomal pH by fluorescence microscopy. *Methods in Cell Biology*. **126**, 85–99 (2015).
26. Armstrong, J. K., Wenby, R. B., Meiselman, H. J., Fisher, T. C. The hydrodynamic radii of macromolecules and their effect on red blood cell aggregation. *Biophysical Journal*. **87**, 4259–4270 (2004).
27. Blum, J. S., Wearsch, P. A., Cresswell, P. Pathways of antigen processing. *Annual Reviews of Immunology*. **31**, 443–473 (2013).
28. Canton, J., Khezri, R., Glogauer, M., Grinstein, S. Contrasting phagosome pH regulation and maturation in human M1 and M2 macrophages. *Molecular Biology of the Cell*. **25**, 3330–3341 (2014).
29. Mantegazza, A. R. et al. NADPH oxidase controls phagosomal pH and antigen cross-presentation in human dendritic cells. *Blood*. **112**, 4712–4722 (2008).
30. Canton, J. et al. The receptor DNGR-1 signals for phagosomal rupture to promote cross-presentation of dead-cell-associated antigens. *Nature Immunology*. **22**, 140–153 (2021).
31. Mishra, R., Bhowmick, N. A. Visualization of macropinocytosis in prostate fibroblasts. *Bio-Protocol*. **9** (2019).
32. Galenkamp, K. M. O., Alas, B., Commisso, C. Quantitation of macropinocytosis in cancer cells. *Methods in Molecular Biology Clifton NJ*. **1928**, 113–123 (2019).
33. Lee, S.-W., Alas, B., Commisso, C. Detection and quantification of macropinosomes in pancreatic tumors. *Methods in Molecular Biology Clifton NJ*. **1882**, 171–181 (2019).

34. Swanson, J. A., King, J. S. The breadth of macropinocytosis research. *Philosophical Transactions of the Royal Society of London B. Biological Sciences*. **374**, 20180146 (2019).

Figure 1

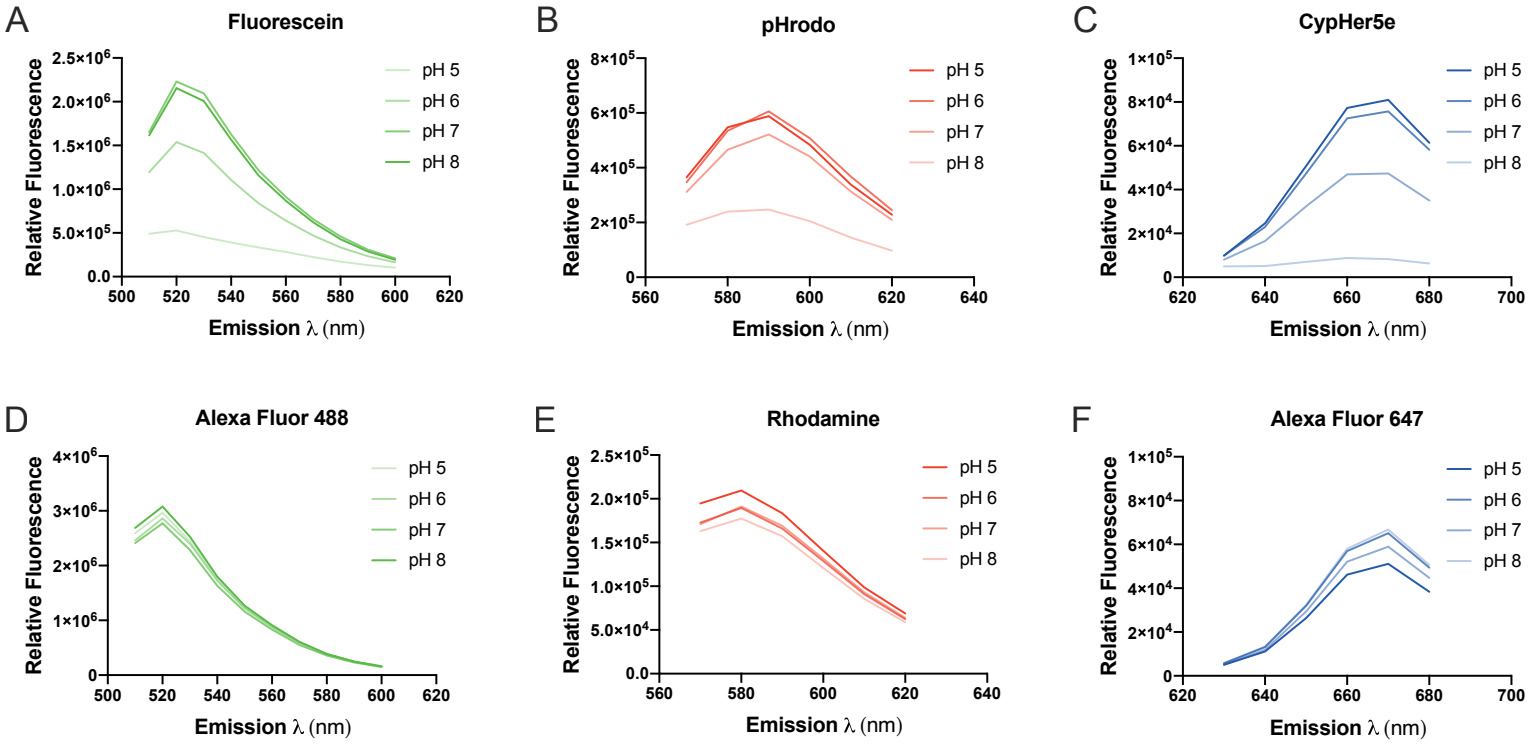

Figure 2

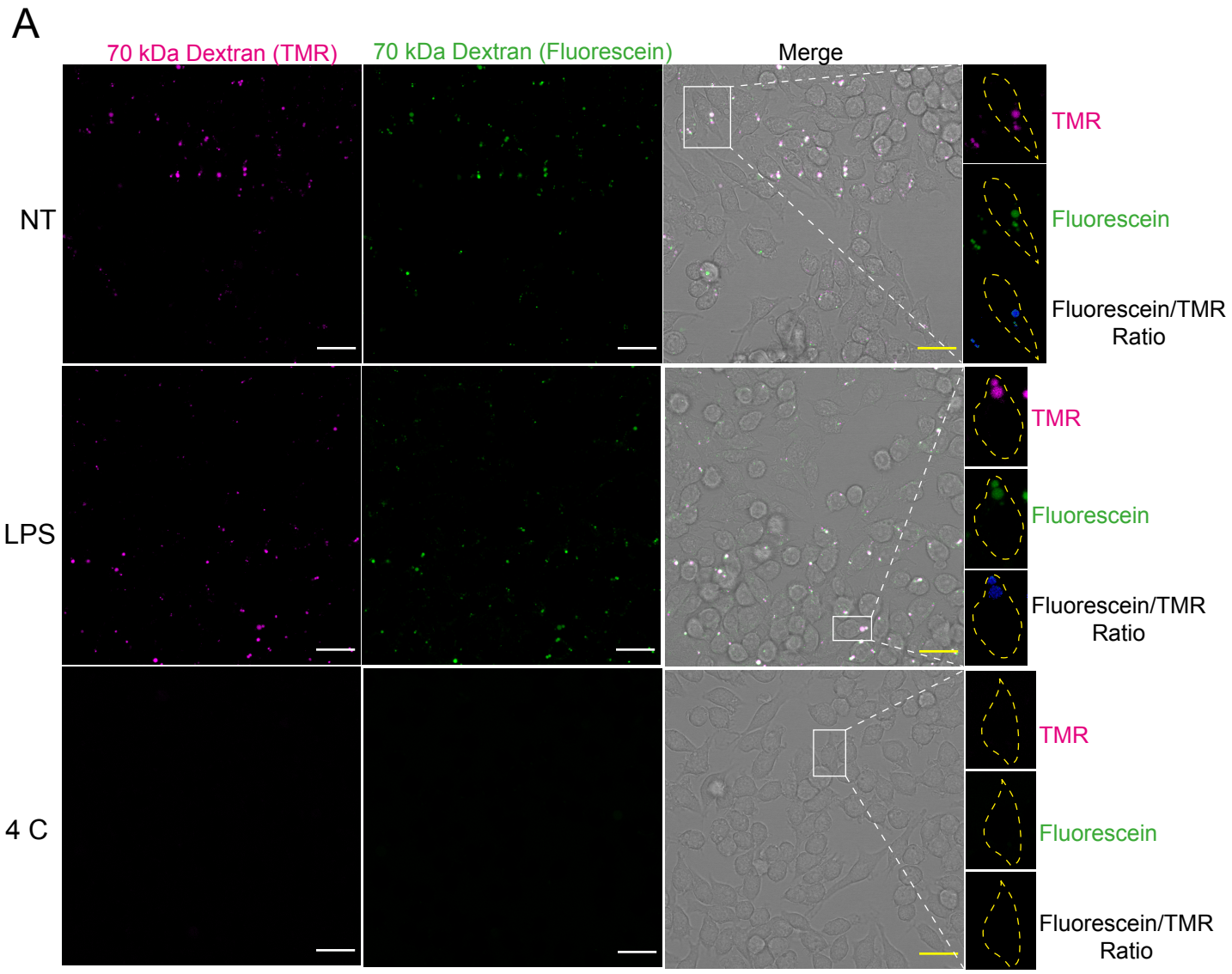

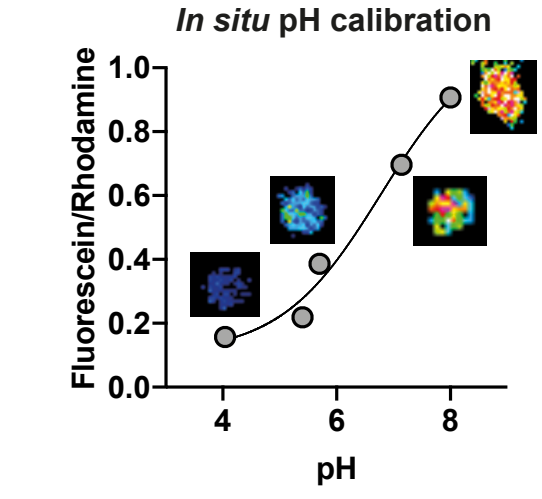

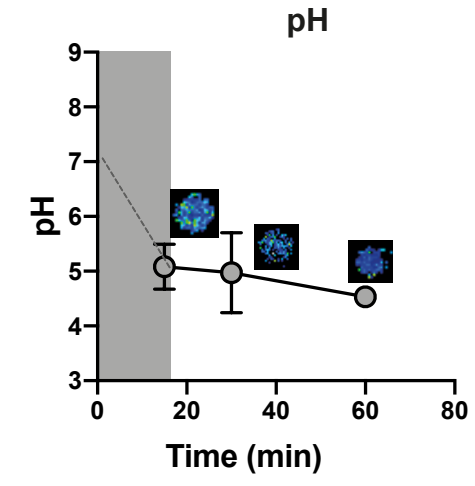

Figure 3

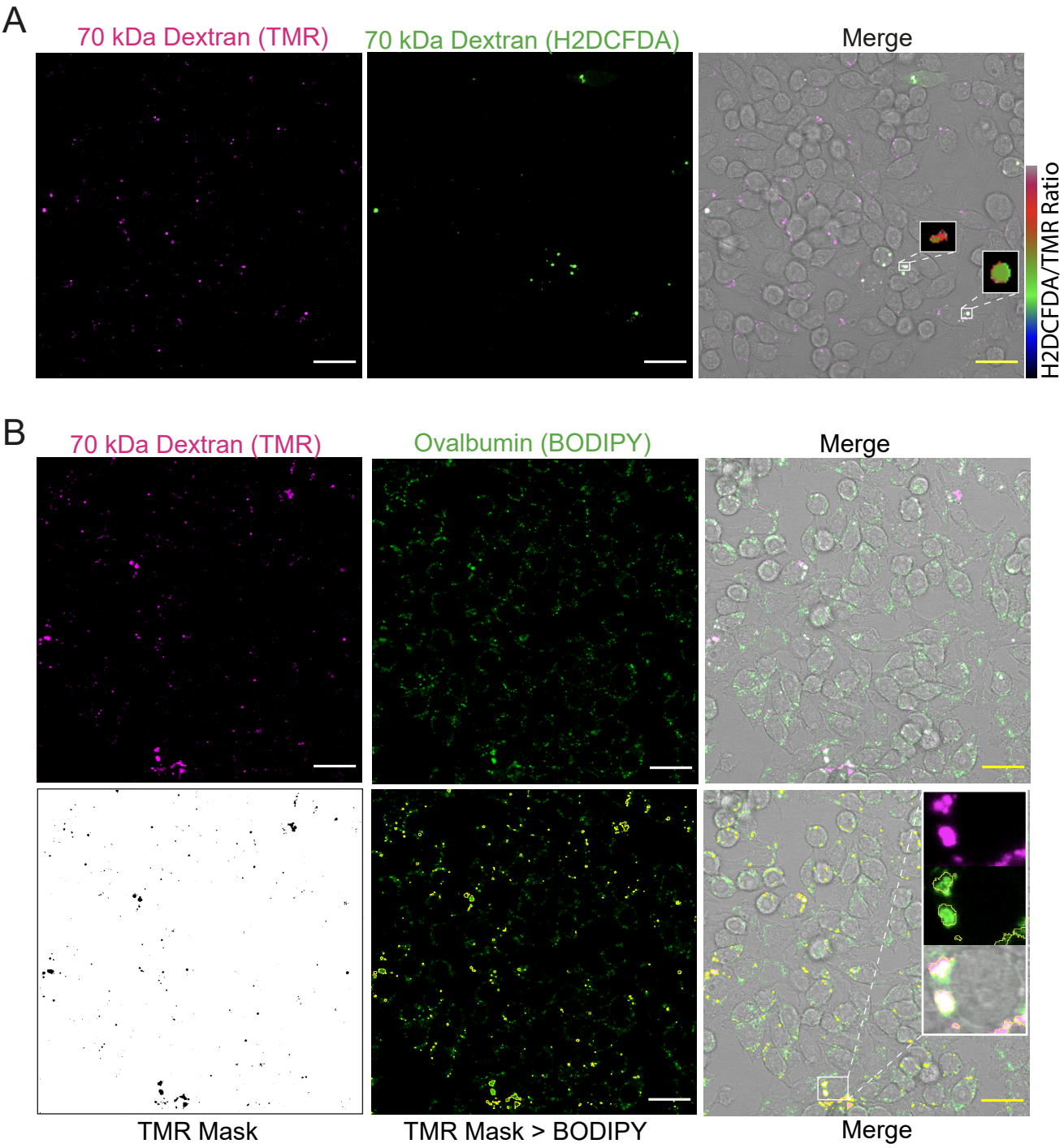

K^+-rich solution	
KCl	140 mM
$MgCl_2$	1 mM
$CaCl_2$	1 mM
D-Glucose	5 mM
HEPES or MES*	25 mM
Nigericin	10 μg/ml

UNIVERSITY OF CALGARY

FACULTY OF VETERINARY MEDICINE

Department of Comparative Biology and Experimental Medicine
Teaching, Research, & Wellness Building (TRW)
2nd Floor, 3280 Hospital Drive NW
Calgary, Alberta T2N4Z6
vet.ucalgary.ca

June 11, 2021

Amit Krishnan
Review Editor
JoVE

Dear Amit:

Please find attached our revised manuscript. We have amended the manuscript with all of the suggestions that you made in our last correspondence. Should any additional edits or information be required please do not hesitate to contact me.

Thank you and we look forward to hearing from you.

Sincerely,
Johnathan Canton